Received: 25 January 2020 | Revised: 5 August 2020 | Accepted: 6 August 2020

DOI: 10.1111/bre.12502

ORIGINAL ARTICLE

Basin Research IAS EAGE WILEY

The importance of trace element analyses in detrital Cr-spinel provenance studies: An example from the Upper Triassic of the Barents Shelf

Trond Svånå Harstad[1] | **Mai Britt Mørk E.**[1] | **Trond Slagstad**[2]

[1]Department of Geoscience and Petroleum, Norwegian University of Science and Technology (NTNU), Trondheim, Norway

[2]Geological Survey of Norway, Trondheim, Norway

Correspondence
Trond Svånå Harstad, Department of Geoscience and Petroleum, Norwegian University of Science and Technology (NTNU), Trondheim, Norway.
Email: trond.s.harstad@ntnu.no

Abstract

Investigations of sandstone provenance often involve U–Pb dating and chemical/mineralogical investigations of detrital minerals that are stable in sediments. As most stable detrital minerals are from felsic–intermediate rocks, investigations of the only mafic–ultramafic mineral considered stable in sediments, chromian spinel (Cr-spinel), can reveal contributions from mafic–ultramafic sources. Cr-spinel chemical compositions are tied to petrogenesis, making it possible to identify the nature of, and differentiate between, potential sources. Earlier detrital Cr-spinel studies have focused on major and minor element compositions, however, the advent of laser-ablation analytical techniques now allow routine mineral trace element analyses. Here, we integrate major, minor and trace element compositions of detrital Cr-spinel from sandstones with a well-characterised provenance from the Triassic (Anisian to Early Norian) Snadd and De Geerdalen formations of the Barents Shelf. The analysed Cr-spinel compositions are depleted in the major element cations Fe^{3+}, Al and Mg and enriched in Cr and Fe^{2+}. Relative to MORB chromite, the minor and trace element data show high concentrations of Zn, Co and Mn, low concentrations of Ni and Ga and variable concentrations of Ti, V and Sc. The major element compositions of the detrital Cr-spinel are similar to ophiolite-associated Cr-spinel, while the trace element compositions indicate a more complex petrogenesis influenced by metamorphic alteration. The compositional variations between sample locations are small, suggesting similar source rocks for the detrital Cr-spinel throughout the study area. The most likely sources of the Cr-spinel grains are metamorphosed ophiolite complexes in the Uralian Orogen, in accordance with earlier provenance studies. The novel addition of trace element compositions to detrital Cr-spinel studies adds significant source-sensitive information.

KEYWORDS

Barents Sea, Cr-spinel, Cr-spinel trace element composition, De Geerdalen Formation, Provenance, Snadd Formation, Tectonics and Sedimentation, Triassic

1 | INTRODUCTION

The chemical composition of detrital Cr-spinel is a favoured provenance method when identifying mafic–ultramafic source rocks (Azizi et al., 2018; Bónová, Mikuš, & Bóna, 2018; Cookenboo, Bustin, & Wilks, 1997). In contrast to common mafic–ultramafic minerals, Cr-spinel is stable in sediments (Morton & Hallsworth, 1999) and variations in Cr-spinel composition related to petrogenesis and tectonic setting make it a useful provenance indicator (Barnes & Roeder, 2001; González-Jiménez et al., 2017; Irvine, 1965; Kamenetsky, Crawford, & Meffre, 2001).

In this contribution, we evaluate detrital Cr-spinel chemical compositions as an important provenance tool in a case study from the Barents Shelf. The correlative, Triassic Snadd and De Geerdalen formations on the Barents Shelf represent an ideal case study for comparing results based on Cr-spinel compositions, as a source has already been suggested from other provenance methods (mainly zircon). Sandstones of the Snadd and De Geerdalen formations contain ubiquitous Cr-spinel, suggesting the presence of mafic–ultramafic source-rock components (Fleming et al., 2016; Mørk, 1999). Furthermore, the sandstone provenance has been investigated in several studies from other locations using different, well-established methods (Bue & Andresen, 2014; Fleming et al., 2016; Flowerdew et al., 2019; Glørstad-Clark, Faleide, Lundschien, & Nystuen, 2010; Khudoley et al., 2019; Klausen, Ryseth, Helland-Hansen, Gawthorpe, & Laursen, 2015; Mørk, 1999; Riis, Lundschien, Høy, Mørk, & Mørk, 2008; Soloviev et al., 2015) suggesting the Uralian Orogen as a predominant source. The Siberian Traps large igneous province (LIP) could be a source of sediment on the Barents Shelf, as suggested by, for example, Zhang, Pease, Skogseid, and Wohlgemuth-Ueberwasser (2016). With the addition of Cr-spinel compositional data, it should be possible to differentiate between a possible ophiolite-related Uralian source and a continental-intrusive Siberian Traps source.

Highlights

- Detrital Cr-spinel chemistry adds significant provenance information about the Snadd and De Geerdalen Formations.
- The novel use of Cr-spinel trace element compositions in a provenance study add source rock information.
- The Cr-spinelchemistry is consistent with a metamorphosed-ultramafic ophiolite complex.
- Consistency in composition throughout the study area suggests a similar source to all samples.
- Consistent with earlier studies, the likely ultimate provenance is the Uralian Orogen.

2 | Cr-SPINEL CHEMISTRY

The informal term Cr-spinel, as used here, describes spinel-group minerals of the general formula AB_2O_4, containing a major proportion of chromium (Irvine, 1965). A wide range of chemical compositions exists within the spinel group due to several possible cation substitutions (Barnes & Roeder, 2001; Dupuis & Beaudoin, 2011). Cations observed to go into the spinel structure are Al^{3+}, Ca^{2+}, Co^{2+}, Cr^{3+}, Cu^{2+}, Fe^{2+}, Fe^{3+}, Ga^{3+}, Ge^{2+}, Mg^{2+}, Mn^{2+}, Mn^{3+}, Ni^{2+}, Sc^{3+}, Ti^{4+}, V^{3+} and Zn^{2+} (Colás et al., 2014; Dupuis & Beaudoin, 2011), with Cr, Fe, Al and Mg being the major elements in Cr-spinel. The original igneous chemical composition of Cr-spinel may become partially or completely altered during metamorphism (Barnes & Roeder, 2001; Colás et al., 2014; Evans & Frost, 1976; Suita & Strieder, 1996). Recognising metamorphic signatures as well as the original igneous composition is, therefore, crucial when interpreting petrogenesis or provenance based on Cr-spinel compositions.

Pristine Cr-spinel of igneous origin in the Earth's crust generally follows two main trends in major element composition: the Cr–Al trend and the Fe–Ti trend (Barnes & Roeder, 2001). Cr-spinel of ophiolitic origin generally follows the Cr–Al trend, characterised by large variation in Cr versus Al concentrations, while the Fe^{3+} and Ti concentrations remain low (Barnes & Roeder, 2001). Continental intrusions follow the Fe–Ti trend and show higher concentrations of Fe^{3+} and Ti. Discrimination diagrams based on empirical data of major element disitibutions can thus be used to disciminate between Cr-spinel originating in continental intrusions and ophiolites, as well as far less abundant Cr-spinel-bearing rocks and subcategories of these (Barnes & Roeder, 2001).

The composition of metamorphically altered Cr-spinel depends on factors such as primary composition, pressure–temperature conditions during metamorphism, composition of fluids and the composition of the host rock (Colás et al., 2014; Fanlo, Gervilla, Colás, & Subías, 2015; Suita & Strieder, 1996), and may also be used to indicate metamorphic grade (Colás et al., 2014; Suita & Strieder, 1996). Alteration of Cr-spinel during metamorphism commonly includes textural alteration and mineral/chemical zoning between core and rim (Colás et al., 2014; Fanlo et al., 2015). The chemical composition of Cr-spinel rims may be significantly altered compared to the cores, commonly with depletion of Al and Mg giving a composition closer to Cr-magnetite (Colás et al., 2014; Suita & Strieder, 1996). In Cr-spinel cores, the degree of major element alteration is less than in the rims, although some loss of Al and Mg, and enrichment of Fe and Cr may occur.

Although there is much less published Cr-spinel trace element data compared to published major and minor element data, compositional variations can be tied to petrogenesis, tectonic setting and alteration (Colás et al., 2014; González-Jiménez et al., 2014, 2015; Pagé & Barnes, 2009; Rui, Jiao, Xia, Yang, & Xia, 2019). Trace element compositions of unaltered ophiolite-related rocks are generally lower in Ga, Ti, Zn, Mn, Co, V and Sc than in layered intrusions (González-Jiménez et al., 2015). Metamorphically altered Cr-spinel displays a varying trace element composition depending on factors such as degree of alteration, original chemistry and type of mineral zoning during alteration. Theoretically, integration of the major, minor and trace element compositions of detrital Cr-spinel should allow us to identify both metamorphic and igneous sources.

3 | GEOLOGICAL SETTING

In the Triassic, the ~1.3 million km^2 Barents Shelf was located north on the supercontinent Pangaea, generally acting as a sediment sink (Bue & Andresen, 2014; Klausen et al., 2015; Lundschien, Høy, & Mørk, 2014; Miller et al., 2013; Riis et al., 2008; Sømme, Doré, Lundin, & Tørudbakken, 2018). A trend of gradual infilling of the basin from the surrounding palaeolands, dominated by a large sediment input from the Uralian orogen, has been inferred in previous studies (Bue & Andresen, 2014; Fleming et al., 2016; Glørstad-Clark et al., 2010; Klausen et al., 2015; Lundschien et al., 2014; Miller et al., 2013; Mørk, 1999; Zhang et al., 2016). Marine conditions dominated early in the period while fluvial and partially erosional reliefs existed at the end of the Triassic (Klausen, Müller, Slama, & Helland-Hansen, 2017; Riis et al., 2008). In the Middle to Late Triassic, deposition of the marginal-marine to fluvial Snadd and De Geerdalen formations represent the last infilling of the palaeobasin (Glørstad-Clark et al., 2010; Klausen et al., 2015; Lundschien et al., 2014).

Various approaches to provenance have suggested that the dominant source of the Snadd and De Geerdalen sandstones was located southeast of the basin, corresponding to an origin from the Uralian Orogen (Miller et al., 2013). Well-documented seismic evidence shows northwestwardly prograding clinoforms filling in the basin at least until Svalbard (Glørstad-Clark et al., 2010; Klausen et al., 2015; Lundschien et al., 2014; Riis et al., 2008). Provenance studies based on detrital minerals, their chemistry, U–Pb ages, occurrence, habitus or combinations of these have generally supported the seismicity-based provenance interpretation (Fleming et al., 2016; Mørk, 1999; Soloviev et al., 2015). Sediment sources other than the Uralian Orogen also existed on the fringes of the palaeobasin (Fleming et al., 2016; Glørstad-Clark et al., 2010), and possibly from palaeohighs within the basin (Mørk, 1999).

The potential source regions, on- and offshore present-day northern Russia, include the Archaean through Proterozoic Baltican and Siberian cratons, reworked in several younger tectonic events. The Uralian Orogen, resulting from Devonian to Permian collision between Baltica and Siberia (Puchkov, 2009), as well as the latest Permian eruptions in the Siberian Traps LIP (Zhang et al., 2016), are plausible sediment sources. The Siberian Traps LIP is characterised by large volumes of mostly mafic igneous rocks. The geology of the Uralian Orogen, as known from the present-day Urals, is characterised by stacked tectonostratigraphic units of foreland sedimentary rocks, pre-Uralian passive-margin sedimentary rocks, pre-collisional continental rocks, several ophiolites and island-arc terranes, and granitic intrusive belts (Puchkov, 2009). The abundance of ophiolitic rocks in the present-day Urals is high compared to other orogenic belts. Triassic tectonism in Taimyr and Novaya Zemlya is often included as a part of the Uralian Orogeny, but these events may be unrelated to the Siberia–Baltica collision (Miller et al., 2013; Zhang, Pease, Carter, Kostuychenko, et al., 2017; Zhang, Pease, Carter, & Scott, 2017).

Petrography and heavy-mineral analyses connect the mineralogically immature arkosic and lithic compositions to the Uralian Orogen (Fleming et al., 2016; Mørk, 1999, 2013). Rock fragments of sedimentary, metamorphic and igneous origin (Fleming et al., 2016; Mørk, 1999), together with distinct proportions of variously altered volcanic rock fragments, are present in the formations (Mørk, 2013). A diverse heavy-mineral assemblage is present in the sandstones, represented by apatite, chloritoid, Cr-spinel, epidote, garnet, rutile, titanite, tourmaline and zircon, supporting the existence of metamorphic, sedimentary and igneous source rocks (Fleming et al., 2016; Mørk, 1999).

Studies focused on detrital zircon ages of the De Geerdalen and Snadd formations describe age distributions that can be associated with the Uralian Orogen (Bue & Andresen, 2014; Fleming et al., 2016; Flowerdew et al., 2019; Soloviev et al., 2015). Detrital zircon ages of sandstones sourced from the Uralian Orogen are dominantly 230–550 Ma, with distinctive peaks at ~235 Ma, ~300 Ma, ~420 Ma and locally at ~550 Ma (Bue & Andresen, 2014; Fleming et al., 2016; Miller et al., 2013). Early Triassic zircon ages were suggested by Fleming et al. (2016) to represent source areas in the northern part of the Uralian Orogen. However, Midwinter, Hadlari, Davis, Dewing, and Arnott (2016) have documented the presence of Triassic-age zircons in Upper Triassic deposits in the Sverdrup Basin, which they attribute to subduction-driven volcanism offshore the Sverdrup Basin. Detrital zircons from the Carnian Osipai Formation, located in the Lena River delta area, display a similar age distribution to those in the Barents Shelf (Letnikova et al., 2014). The ~235 Ma age peak present in these data is associated with local

volcanism (Letnikova et al., 2014). Detrital Cr-spinel compositions from the same formation suggest that the Siberian Traps LIP is a major source (Nikolenko et al., 2018).

4 | SAMPLE LOCATIONS AND SANDSTONE COMPOSITION

The studied locations (Figure 1 and Table 1) in the Barents Sea define a northeast–southwest transect from the Sentralbanken High to the Nordkapp Basin based on shallow stratigraphic drill cores obtained by the Continental Shelf Institute (IKU, present-day SINTEF Petroleum) and the Norwegian Petroleum Directorate (NPD) (Bugge et al., 2002; Lundschien et al., 2014). The Snadd formation in the Barents Sea cores is correlated with comparable sedimentary units of the De Geerdalen Formation in outcrops on Svalbard (Lundschien et al., 2014; Vigran, Mangerud, Mørk, & Hochuli, 2014). The study area in the Nordkapp Basin is within the south-eastern part of the prograding deltaic succession (e.g. Bugge et al., 2002). Studied samples from the Nordkapp Basin represent sediments from barrier, shoreface, marginal-marine and delta-plain environments (Bugge et al., 2002). Similar delta-plain environments are inferred for the Snadd formation at the Sentralbanken High and the Bjarmeland Platform (Lundschien et al., 2014; Stensland, Auset, Elvebakk, & Mørk, 2013), as well as for the same stratigraphic level in the De Geerdalen

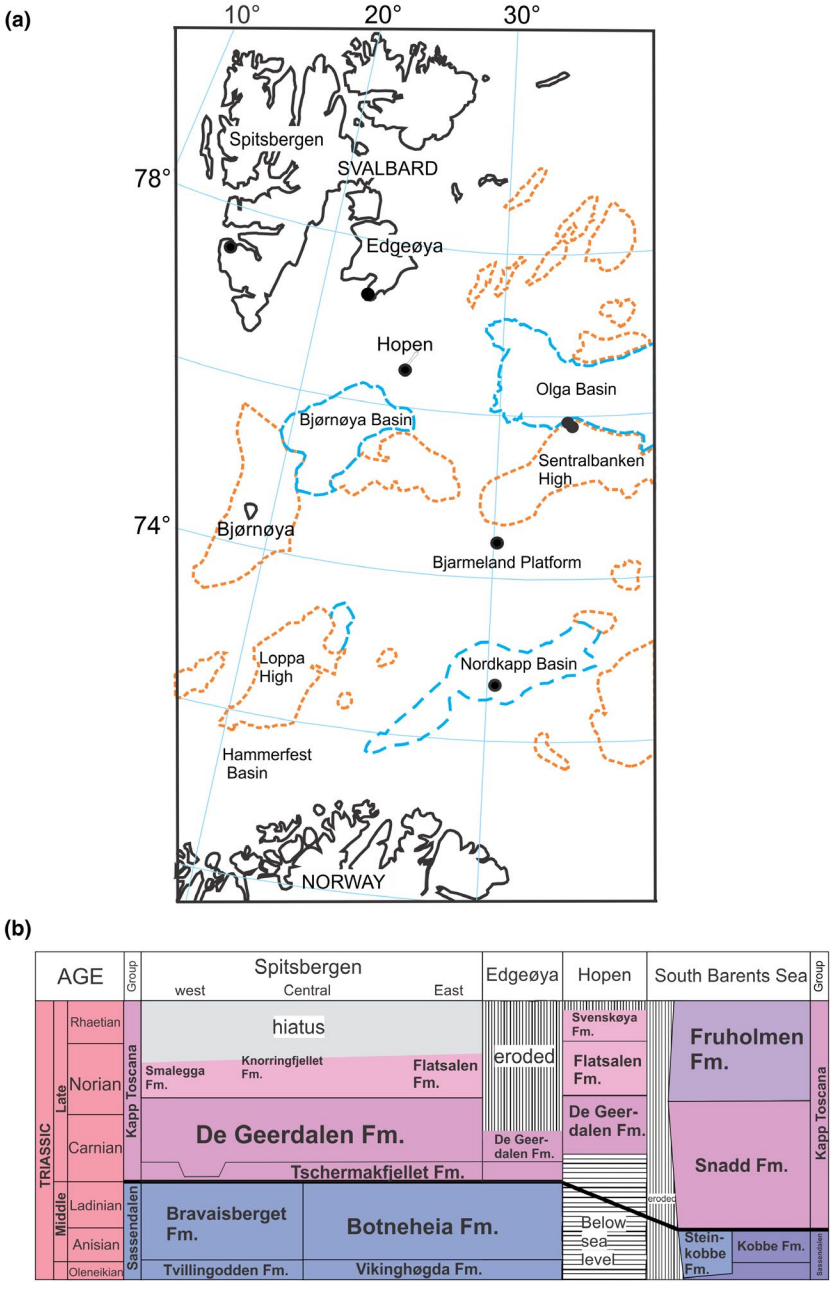

FIGURE 1 (a) Map of the Norwegian Barents Shelf with outlines of structural highs and basins, map modified from Lundschien et al. (2014). Sample locations are indicated with black points. (b) Lithostratigraphic overview of the Triassic of the sampled area (Lundschien et al., 2014)

TABLE 1 Sample locations and number of Cr-spinel grains included for major and trace element analysis

Area and formation		Stratigraphic age (Vigran et al., 2014)	Core number	Depth below seafloor	*N* grains EPMA	*N* grains LA-ICP-MS
Barents Sea, Snadd Fm.	Nordkapp Basin	Late Carnian	7230/05-U-03	114 m	33	20
		Ladinian	7230/05-U-05	33 m	42	33
			7230/05-U-05	38 m	35	19
	Bjarmeland Platform	Early-mid Carnian	7430/07-U-01	56 m	36	20
	Sentral-banken High	Early Carnian	7533/02-U-01	46 m	31	26
			7533/02-U-01	123 m	24	15
			7533/03-U-07	111 m	30	21
			7533/03-U-07	147 m	23	14
Svalbard		Sample/Location				
De Geer-dalen Fm.	Hopen	Carnian (?)	H30 EO25	UTM35	52	31
	Edgeøya	Carnian (?)	KTO12	X0446533	36	27
	Spitsbergen	Carnian/		Y8487870	37	23
		Norian (?)		UTM35		
				X0395946		
				Y8585416		
				UTM33		
				X0501340		
				Y8608640		

Abbreviations: EPMA, electron probe microanalyser; LA-ICP-MS, laser-ablation inductively coupled plasma mass spectrometry.

Formation onshore Svalbard (Vigran et al., 2014); the latter is sampled at three locations: Hopen, Edgeøya and near van Keulenfjorden in southwest Spitsbergen (Figure 1, Table 1). Stratigraphic columns showing sample locations at Hopen and Edgeøya are included in Supplements A and B respectively.

Samples come from channel and barrier deposits of moderately to well-sorted, fine- and medium-grained sandstone. The sampled rock intervals comprise mineralogically immature lithic and arkosic arenites, as described in the literature (Mørk, Knarud, & Worsley, 1982; Mørk, 1999, 2013; Riis et al., 2008). The main detrital components are quartz, K-feldspar, plagioclase, mica, abundant cherty rock fragments as well as lithic clasts of altered volcanic/igneous, metamorphic and recycled sedimentary rocks. Accessory heavy minerals include Cr-spinel, zircon, garnet, tourmaline and opaque minerals (Mørk, 1999; Riis et al., 2008). Notably, the sandstones from shallow core sites have experienced less burial compared to studied locations in western Spitsbergen, where net erosion is estimated to be more than 2.5 km (Henriksen et al., 2011).

5 | METHOD

Cr-spinel compositions from 11 sandstone samples from the Snadd and De Geerdalen formations were analysed, representing three areas in the Norwegian Barents Sea and three locations onshore Svalbard. Offshore cores were drilled by the NPD and IKU/SINTEF Petroleum, while the onshore Svalbard samples were collected during an NPD and SINTEF expedition to Svalbard in August 2014. Further information about the analysed samples is found in Table 1. The samples were crushed and dry sieved before cleaning for fine particles with water to obtain the 37–250 μm fraction. Cr-spinel was separated from the sandstone fraction by heavy-liquid (diiodmethane, 3.325 g/ml) separation and handpicked using tweezers under a binocular microscope. Grains were mounted in epoxy and polished to expose their interiors. A 1450VP Scanning Electron Microscope (SEM) from LEO Electron Microscopy LTD at the Geological Survey of Norway, Trondheim, was used to image the grains prior to analysis and identify any compositional variation within the mounted Cr-spinel grains.

Major and minor element concentrations were obtained by wavelength-dispersive spectroscopy (WDS). X-ray analyses on a JEOL JXA–8200 Superprobe electron probe microanalyser (EPMA) equipped with 5 WDS spectrometers, using Probe for EPMA™ microanalysis software, at Dalhousie University, Halifax, Canada. All analyses were performed using an acceleration voltage of 15 kV, analytical beam current of 20 nA and beam diameter of 1 μm, with an X-ray take-off angle of 40°. In all cases, the Kα X-ray for each element was analysed. For V, Mg, Si, Fe, Cr, Mn, Al, Ni and Zn, peak counting times were 20 s, with 10 s upper- and lower-background counting times; for Ti, the peak counting time was 30 s, with 15 s background counting times. The following standards were used for data reduction: Ti – rutile, V – V metal, Mg, Fe, Cr, Al – chromite, Si – sanidine, Mn – pyrolusite, Ni – Ni metal and Zn

– willemite. At regular intervals, analyses of known chromite and magnetite standards were performed for quality control. Ferrous and ferric proportions of Cr-spinel were then calculated assuming spinel stoichiometry, following Droop (1987) and Barnes and Roeder (2001).

The Cr-spinel grains were analysed for trace element compositions using the laser-ablation inductively coupled plasma mass spectrometry (LA–ICP–MS) instrument at the Aarhus Geochemistry and Isotope Research platform (AGIR), Department of Geoscience at Aarhus University, Denmark. The LA–ICP–MS setup consisted of a 193 nm Excimer laser from Resonetics attached to an Agilent 7,900 quadrupole ICP–MS. The analyses were carried out on the grain mounts with single-spot ablations and spot sizes of 18, 26 and 40 μm, depending on grain size. Helium was used as the carrier gas, which was mixed with Ar before it entered the ICP. The measurements included 25 s of background and 35 s of ablation. The ablation rate was 8 Hz and the energy 80 mJ. The NIST 610 reference material was used as the external calibration standard (Jochum et al., 2006), while NIST 612 and magnetite BC–28 from Bushveld were used as secondary standards. The data processing and quantification were done in Iolite (Paton, Hellstrom, Paul, Woodhead, & Hergt, 2011). The internal standard for the quantification was Cr, the concentration of which was determined by microprobe analysis. The elements Al, Co, Cu, Fe, Ga, Mg, Mn, Nb, Ni, Pb, Sc, Ti, V and Zn were measured with a dwell time of 10 ms per mass. Detection limits for each element were calculated as 3 sigma standard deviation of the background counts. Analyses where the detection limit overlaps 2 sigma uncertainty of the reported concentration were discarded. The geochemical data are listed in Supplements C and D.

6 | RESULTS

We performed 626 EPMA analyses of 581 Cr-spinel grains from 11 samples. SEM images and 45 grain centre–edge analyses show that the mounted grains are generally homogenous. Chemical variation was observed in less than 5% of the grains. The few grains displaying chemical variation did not have zoning textures, but rather thin lines resembling filled cracks. For each sample, 40–60 Cr-spinel mineral grains were analysed using EPMA. Of these, between 18 and 35 grains were analysed by LA–ICP–MS for trace element composition. Three hundred and eighty EPMA analyses were deemed to have acceptable totals within ±1% of the observed total in the chromite reference material of 99.6%, whereas 241 acceptable LA–ICP–MS analyses were obtained. Concentrations of particular elements from EPMA and LA–ICP–MS analyses (included in Supplement E) generally display linear trends in XY plots, indicating that the data obtained with the two methods are comparable. The mineral chemical results for all samples are illustrated in Figures 2–7.

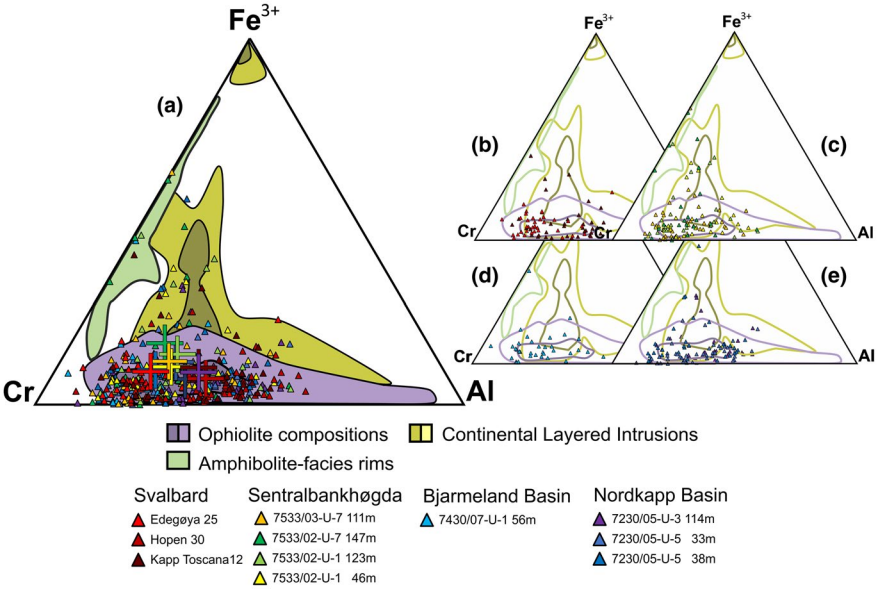

FIGURE 2 Triplot of the trivalent cations Cr, Fe^{3+} and Al in Cr-spinel, compared to the density distributions percentiles of Barnes and Roeder (2001) and the amphibolite-facies rim distribution of Colás et al. (2014). Note that the amphibolite-facies rim distributions do not have distribution percentiles, as they are based on less data. Individual triangles represent single-grain compositions; crosses represent average composition of each sample. (a) All compositional plots, (b) Svalbard analyses, (c) Sentralbankhøgda analyses, (d) Bjarmeland Platform analyses and (e) Nordkapp Basin analyses. The vast majority of the detrital Cr-spinel analyses plot within the density distribution of ophiolitic Cr-spinel, independent of sample location. Darker shades within the density distribution diagrams represent the 50th percentile, lighter shades represent the 90th percentile

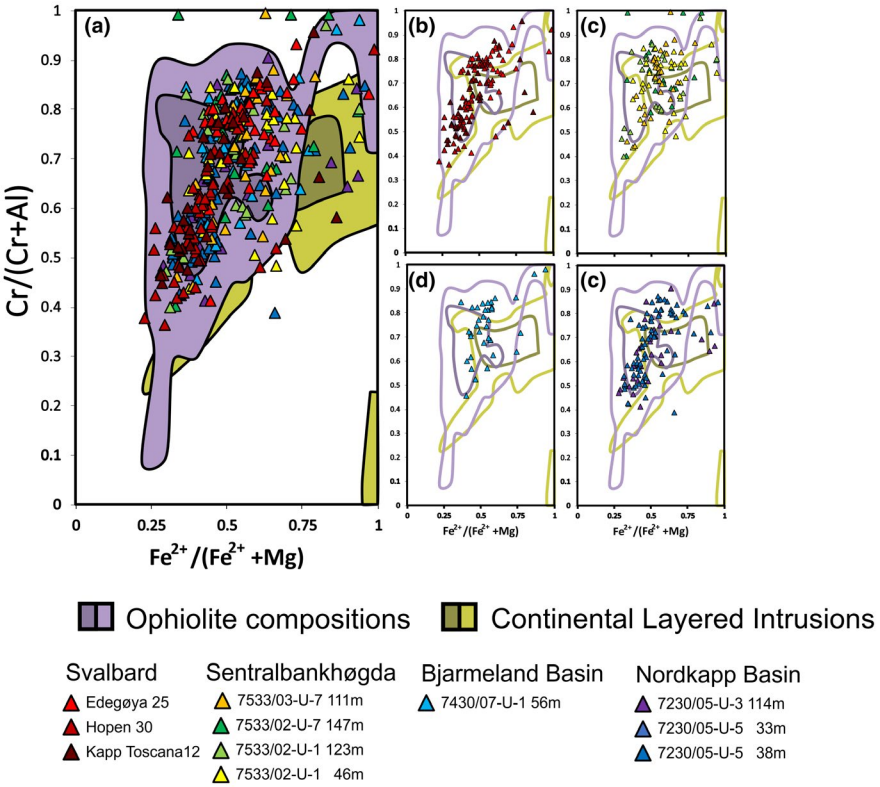

FIGURE 3 Comparison of $Fe^{2+}/(Fe^{2+} + Mg)$ versus Cr# to the density distributions of ophiolites and layered intrusions. (a) All compositional plots, (b) Svalbard analyses, (c) Sentralbankhøgda analyses, (d) Bjarmeland Platform analyses and (e) Nordkapp basin analyses. The analyses generally plot within the ophiolite field

The data show a large degree of consistency between samples, independent of variables such as location or depositional age. Average chemical compositions are similar and while variation within each sample is considerable, the scatter is similar for all the samples. Normalising the dataset to chromite/chromitite in MORB, as in Pagé and Barnes (2009), shows that concentrations of Al, Ga, Ti, Ni and Mg are low compared to the reference dataset. The average concentrations for these elements are 15.3 wt% Al_2O_3, 38.5 ppm Ga, 1,280 ppm Ti (LA–ICP–MS data), 728 ppm Ni and 9.9 wt% MgO. Zn, Co, Mn, Fe, Sc and Cr have high concentrations, with averages of 4,356 ppm Zn, 546 ppm Co, 3,312 ppm Mn, 24.9 wt% FeO^{tot}, 6.49 ppm Sc and 47.7 wt% Cr_2O_3. V content is close to the reference value with an average of 1,446 ppm. Other trace elements present in some of the grains are Cu, Nb and Pb. The Cr-numbers (Cr# = Cr/(Cr + Al)) range from 0.36 to 1.0 with an average of 0.68; 86% of the analyses plot between 0.50 and 0.87. Fe^{3+} concentrations are mostly low, with Fe^{3+} numbers ($Fe^{3+}\# = Fe^{3+}/(Fe^{3+} + Cr + Al)$) (mol %) ranging between 0 and 0.63 with an average of 0.09; 90% of the grains have values between 0 and 0.18. Mg and Fe^{2+} concentrations vary considerably, with Mg numbers ($Mg\# = Mg/(Mg + Fe^{2+})$) ranging between 0.23 and 0.99, averaging 0.52; 90% of the analysis have values between 0.31 and 0.74. TiO_2 concentrations range from 0 to 2.24 wt% with an average of 0.16 wt%; 90% of the grains have a TiO_2 concentration below 0.45 wt%.

6.1 | Major element compositions and plots

Figure 2 compares the major element trivalent cation compositions to known chemical compositional fields (Barnes & Roeder, 2001; Colás et al., 2014) of Ophiolitic, Layered intrusions and metamorphic Cr-spinel. Ninety per cent of the Cr-spinel grains plot within the empirically defined density distribution of ophiolitic Cr-spinel characterised by variable Al and Cr content and generally low Fe^{3+} content. The Fe^{3+} concentration in ophiolite-hosted spinel can reach up to 20% of the trivalent cations. Mineral grains containing higher proportions of Fe^{3+} plot within several possible fields, such as those of continental layered intrusions. A few Cr-spinel analyses plot outside of the ophiolite field, but the considerable overlap of compositional fields necessitates comparison in other discrimination plots. A small, but characteristic group of Cr-spinel grains has a chemical composition corresponding to amphibolite-facies magnetite rims, an indication of metamorphic conditions in the source area.

The diagram Cr# versus $Fe^{2+}/(Fe^{2+}+Mg)$ (Figure 3) is also conventionally used when determining Cr-spinel petrogenesis (Barnes & Roeder, 2001). We observe a compositional trend with relatively high to low Al and Mg content. This trend corresponds well to Cr-spinel of ophiolitic origin, with only 6% of the individual Cr-spinel grains plotting outside the distribution of ophiolites (Barnes &

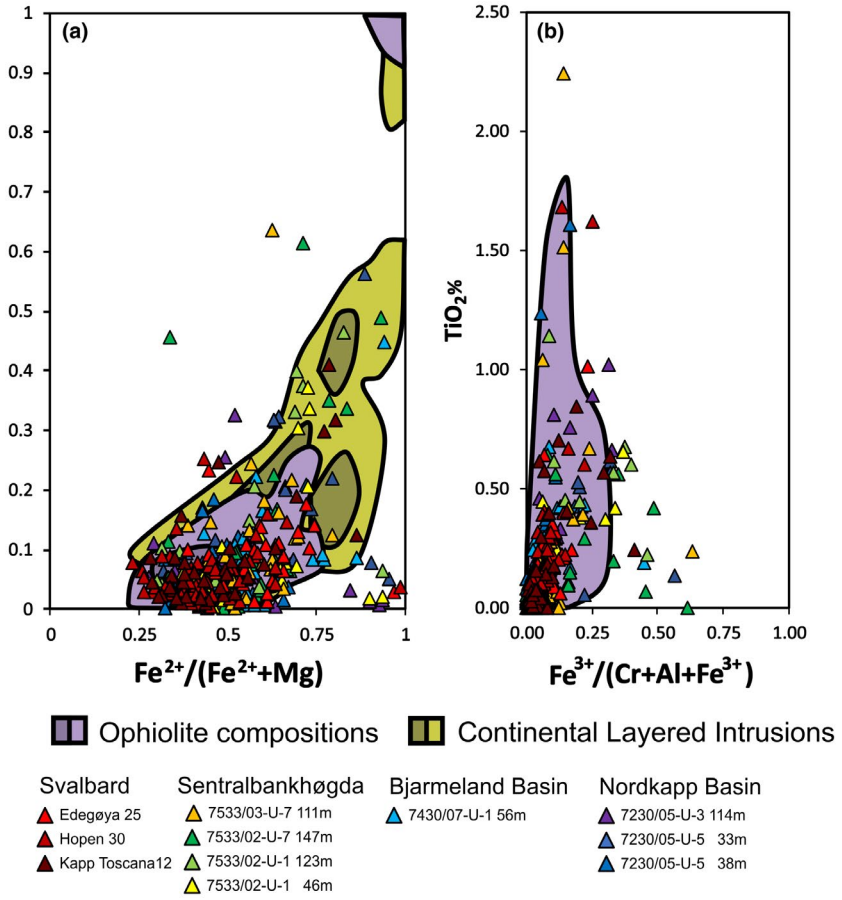

FIGURE 4 Comparison of (a) $Fe^{2+}/(Fe^{2+} + Mg)$ versus $Fe^{3+}/(Cr + Al + Fe^{3+})$ and (b) $Fe^{3+}/(Cr + Al + Fe^{3+})$ versus TiO_2, to the density distributions of ophiolites and layered intrusions. Individual grains plot within the density distribution of ophiolites

Roeder, 2001). A considerable overlap in composition of Alaskan–Uralian type and Stratiform complexes is evident, especially for the Fe^{3+}-enriched Cr-spinel grains. The Fe^{3+}-enriched grains do not overlap the typical island-arc distributions, making continental, intrusive mafic–ultramafic magmatic rocks (e.g. layered intrusions, flood basalts and subvolcanic intrusions) a likely source for these grains. In the Fe^{3+}# versus $Fe^{2+}/(Fe^{2+}+Mg)$ diagram (Figure 4a), the vast majority of Cr-spinel grains show ophiolitic compositions, with a small Fe^{3+}-rich subset largely plotting within the field of continental mafic–ultramafic layered intrusions. In a plot of TiO_2 wt% versus Fe^{3+}# (Figure 4b), 94% of the analyses plot within the field of ophiolitic Cr-spinel compositions, in accordance with observations in other discrimination diagrams.

The plot in Figure 5 subdivides the Cr-spinel grains into the sources' potential tectonic setting, as suggested by Kamenetsky et al. (2001). Here, the Cr-spinel compositions plot throughout the Supra-Subduction-Zone (SSZ) Peridotite field, with only a few grains falling outside this compositional field. A considerable proportion of the Cr-spinel grains in this study have Ti concentrations that are too low to be included in Figure 5. A SSZ Peridotite appears a likely source based on the Cr-spinel grains that plot within the diagram.

6.2 | Trace element composition

In Figure 6, Cr-spinel major, minor and trace element compositions have been normalised to the chromite/chromitite-in-MORB values of Pagé and Barnes (2009). There is significant variation within each sample (Figure 6a), but the averages of each sample show consistent and similar patterns (Figure 6b). Compositional variation is most evident in the normalised Ti concentrations, which vary by three orders of magnitude. For the other trace and minor elements, the variations are typically within one order of magnitude.

The relative depletion of Al, Ga, Ni and Mg, together with the relative enrichment of Zn, Co, Mn, Fe and Cr, is likely the result of metamorphic alteration of Cr-spinel, with individual detrital grains representing varying degrees of chemical alteration (Colás et al., 2014; Fanlo et al., 2015; Rui et al., 2019). As documented by Colás et al. (2014), the trace element compositions in Cr-spinel vary within each mineral grain, depending on the metamorphic history and the type of host rock (Rui et al., 2019; Anna Pryadunenko personal communication). Trace and minor elements appear to be much more affected by metamorphism and alteration than the major elements (Colás et al., 2014).

Processes related to various degrees of metamorphic alteration, as well as alteration in the diagenetic sedimentary

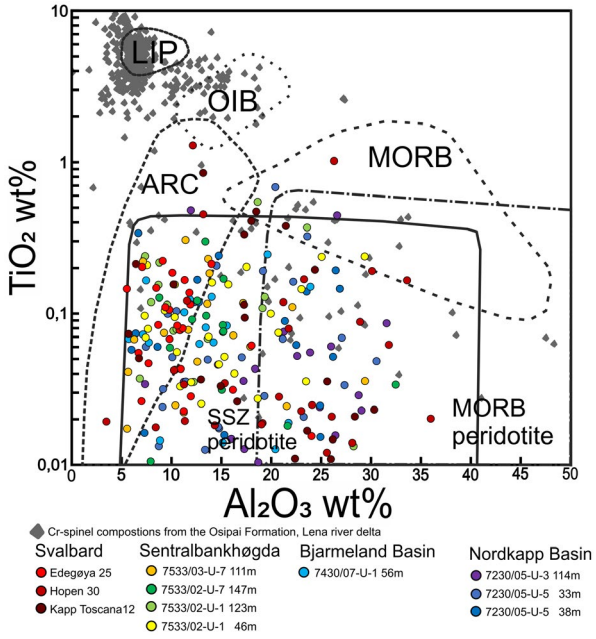

FIGURE 5 Distribution of the De Geerdalen and Snadd formations Cr-spinel grains in a Al_2O_3 wt% versus TiO_2 wt% plot compared to the distributions of Kamenetsky et al., (2001), along with detital Cr-spinel from the Carnian Osipai Formation in the Lena Delta area (Nikolenko et al., 2018). Only a minor portion of individual grains from the Barents Shelf plot outside the compostional space expected for Supra-Subduction-Zone Peridotites. In contrast, the coeval Osipai Formation received detritus from the Siberian Traps LIP. ARC, Island Arc; LIP, Large Igenous Province; MORB, Mid-Ocean Ridge Basalt; OIB, Ocean Island Basalt; SSZ, Supra-Subduction Zone

system, can explain the chemical variation between different Cr-spinel grains within each sample. Various degrees of alteration within each mineral grain and between adjacent minerals in the source rock affect the composition of the investigated detrital grains. Sorting as well as mechanical and chemical alteration have also affected the detrital Cr-spinel grains studied here. In Figure 6b, it can be noted that the average composition of the Snadd and De Geerdalen formation Cr-spinel samples all plot between compositions of altered and partially altered Cr-spinel cores (grey area).

Several of the Cr-spinel grains in the Snadd and De Geerdalen formations have values that are clearly related to metamorphic alteration. Most of the mineral grains do, however, have concentrations between the fields of partially and completely altered Cr-spinel compositions (Figure 7). Figure 7 compares trace and minor element compositions with the Cr# and shows that Ga and Ni (Figure 7a,c) concentrations have negative trends versus Cr#, while Ti (Figure 7b) shows both a Ti-poor population and a population of scattered, Ti-rich grains. The elements Zn, Co and Mn (Figure 7d–f) are significantly more prevalent than expected in unaltered Cr-spinel (González-Jiménez et al., 2015, 2017), but generally have concentrations lower than reported in, for example, altered cores of zoned chromite (Colás et al., 2014; Rui et al., 2019). V and Sc concentrations (Figure 7g,h) are somewhat enriched compared to the unaltered Cr-spinel fields. Higher Fe^{3+} concentrations appear to correlate well with high element concentrations of Ga, Ti, Ni and Sc (Figure 7a–c,h). The other elements in Figure 7 show no covariation with Fe^{3+} concentration. Rui et al. (2019)) show that Sc and V concentrations vary in Cr-spinel between different ophiolite-related, Cr-spinel-bearing rock types. The highest Sc concentrations are found in dunite, suggesting a possible source of the Sc-enriched, detrital Cr-spinel in this study.

7 | DISCUSSION

Comparisons of Cr-spinel compositions from the Snadd and De Geerdalen formation sandstones on the Barents Shelf suggest a metamorphosed ophiolitic source. Conventional major and minor element discrimination diagrams indicate ophiolitic and Supra-Subduction-Zone signatures, while the addition of trace element data shows that the detrital Cr-spinel grains are metamorphosed (Figures 6 and 7). These features suggest that the term 'metamorphosed ophiolite' best describes the source. We experienced challenges in interpreting provenance when only applying conventional major and minor element compositional diagrams. When we included the trace element compositions, a more detailed picture emerged, adding significant provenance-sensitive information. Here, we discuss both the source of the detrital Cr-spinel grains of our case study and evaluate the novel use of trace elements in detrital Cr-spinel provenance analysis.

7.1 | Cr-spinel provenance of the Snadd and De Geerdalen formations

The detrital Cr-spinel grains in the Snadd and De Geerdalen formations have chemical compositions consistent with provenance from a region containing metamorphosed ophiolites. Overlapping compositional variation and average concentrations suggest the same Cr-spinel provenance for all samples. Regional variations are not apparent in the dataset, suggesting continuous erosion and deposition of the same types of mafic–ultramafic source rocks or sedimentary reworking of units derived from these sources. The Cr-spinel chemistry is consistent with earlier interpretations of a provenance from the Uralian Orogen (Fleming et al., 2016; Klausen, Nyberg, & Helland-Hansen, 2019; Klausen et al., 2015; Lundschien et al., 2014; Miller et al., 2013; Mørk, 1999; Riis et al., 2008), which contains substantial volumes of metamorphosed, ophiolite-related ultramafic rocks (e.g. Garuti, Pushkarev, Thalhammer, & Zaccarini, 2012). A comparison of our dataset to the Osipai Formation detrital Cr-spinel in

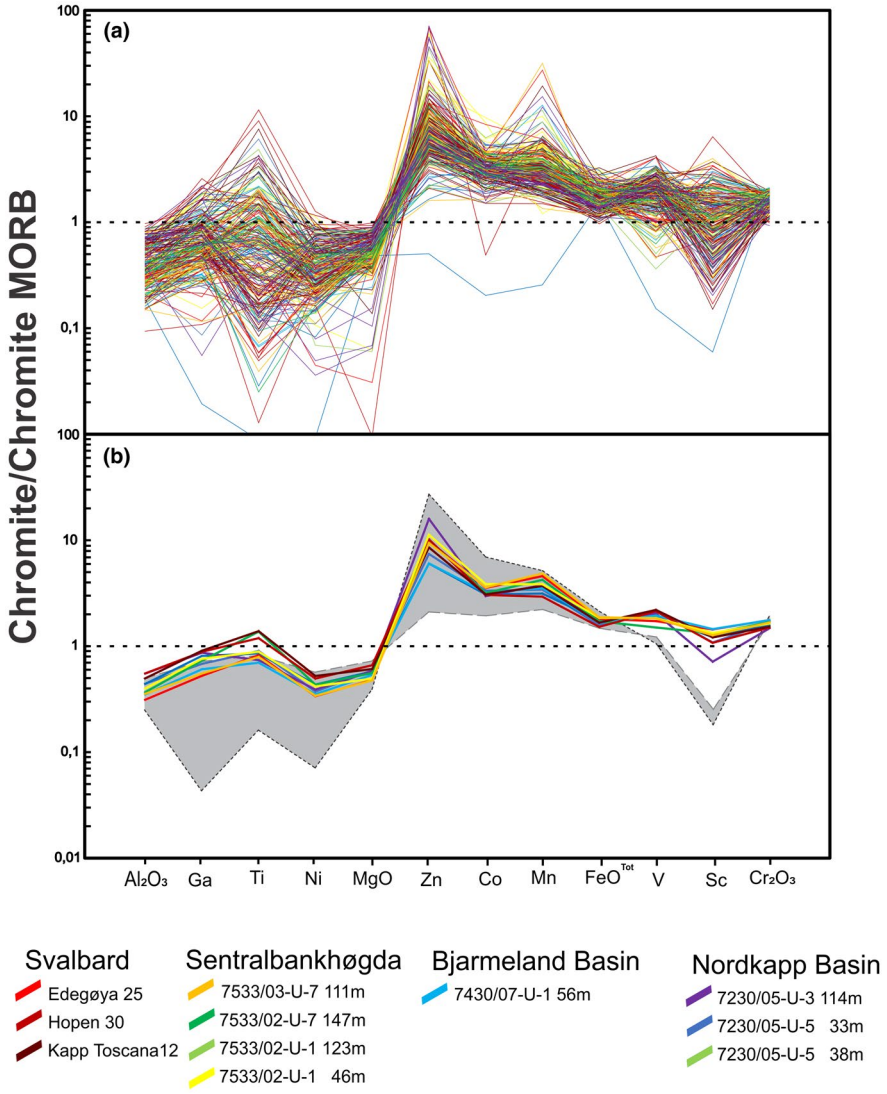

FIGURE 6 Major, minor and trace element compostions of the Snadd and De Geerdalen formations Cr-spinel analyses normalised to the chromite/Chromitite in MORBvalues of Page et al. (2009). (a) Plot of all 241 grains with available trace element data; the samples display a varied compositional distribution. A general trend of low Al, Ga, Ni and Mg as well as high Zn, Co, Mn, Fe, V and Cr is observed; Ti and Sc vary considerably and V displays some variation. (b) Average normalised values of each sample are shown to be similar and follow the same patterns; this is also true for the elements displaying the most scatter in (a). The gray area represents the compositional area between altered cores (black dotted line) and partially altered cores (grey stiped line) as calculated from average compostions in Colás et al. (2014) and Rui et al. (2019)

Figure 5 illustrates the difference between Cr-spinel compositions from sedimentary rocks on the Barents Shelf and those expected from a LIP. As such, there is no indication of influx of material from the Siberian Traps LIP or an island-arc terrane in the Cr-spinel chemical data in this study. A metamorphosed source is consistent with petrographic analyses by, for example, Mørk (1999) and Fleming et al. (2016), who identified high proportions of metamorphic minerals and lithic fragments in Snadd formation detritus. There is also a considerable proportion of Ti oxides, garnet and epidote of potentially metamorphic origin in the sediments (Fleming et al., 2016; Mørk, 1999).

Alternative source regions to the Uralian Orogen would include the cratons of Baltica and Laurentia, both containing various ultramafic rocks (Hölttä et al., 2008; Säntti, Kontinen, Sorjonen-Ward, Johanson, & Pakkanen, 2006), as well as the metamorphosed ultramafic rocks in the Caledonian Orogen (Moore & Qvale, 1977). The volume of Cr-spinel-bearing rocks is, however, lower in these potential sources, when compared to the large area of exposed ultramafic rocks in the present-day Urals. Neoproterozoic ophiolites in Taimyr (Priyatkina et al., 2017) represent another potential source, although less voluminious. In the Polar Urals, the large ophiolite-related ultramafic complexes of Ray–Iz and Voykar–Syninsky represent two of the possible sources (Garuti et al., 2012).

The consistent Cr-spinel composition differs somewhat from provenance interpretations based on detrital zircon age distributions, as described, for example, on Svalbard and in the southern Barents Sea (Bue & Andresen, 2014; Fleming et al., 2016). While the Cr-spinel source remains stable, the detrital-zircon age distribution changes during the depositional history. The difference in Cr-spinel and zircon provenance may represent an evolution or a change in the zircon source. The zircon data seem to indicate a mixed or changed sediment influx better than Cr-spinel, possibly because of the more common occurrence of zircon in a range of potential source rocks. The Cr-spinel compositions of this study identify the presence of the metamorphosed ophiolitic Cr-spinel in the sediments, while other sediment sources are not

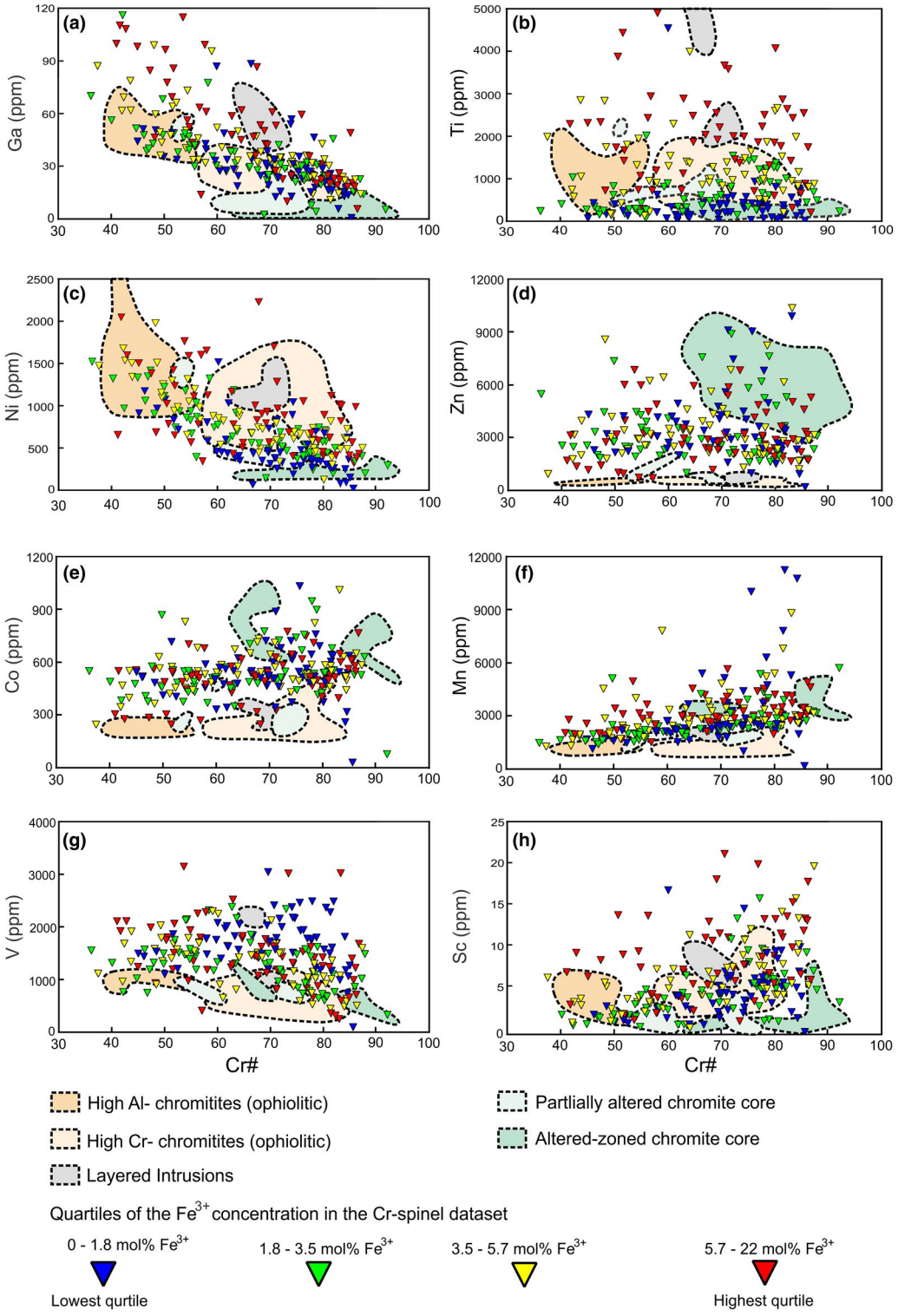

FIGURE 7 Plots of trace element concentrations versus Cr#, compared to distributional fields of podiform chromitites (high Al and Cr) and layered intrusions, as presented by González-Jiménez et al. (2017) and fields for altered grain cores based on data from Colás et al. (2014) and Rui et al. (2019). The values are sorted in quartiles according to Fe^{3+} concentrations. Ga and Ni are negatively correlated with Cr#, whereas Ti is either very low or strongly scattered. Zn, Co and Mn have high concentrations and a small positive correlation with Cr#. V and Sc have high concentrations and are not correlated with Cr#. Ga, Ti, Ni and Sc values generelly show positive covariance, Ti being the element where this is clearest. Zn, Co, Mn and V values seem independent of Fe^{3+} concentrations

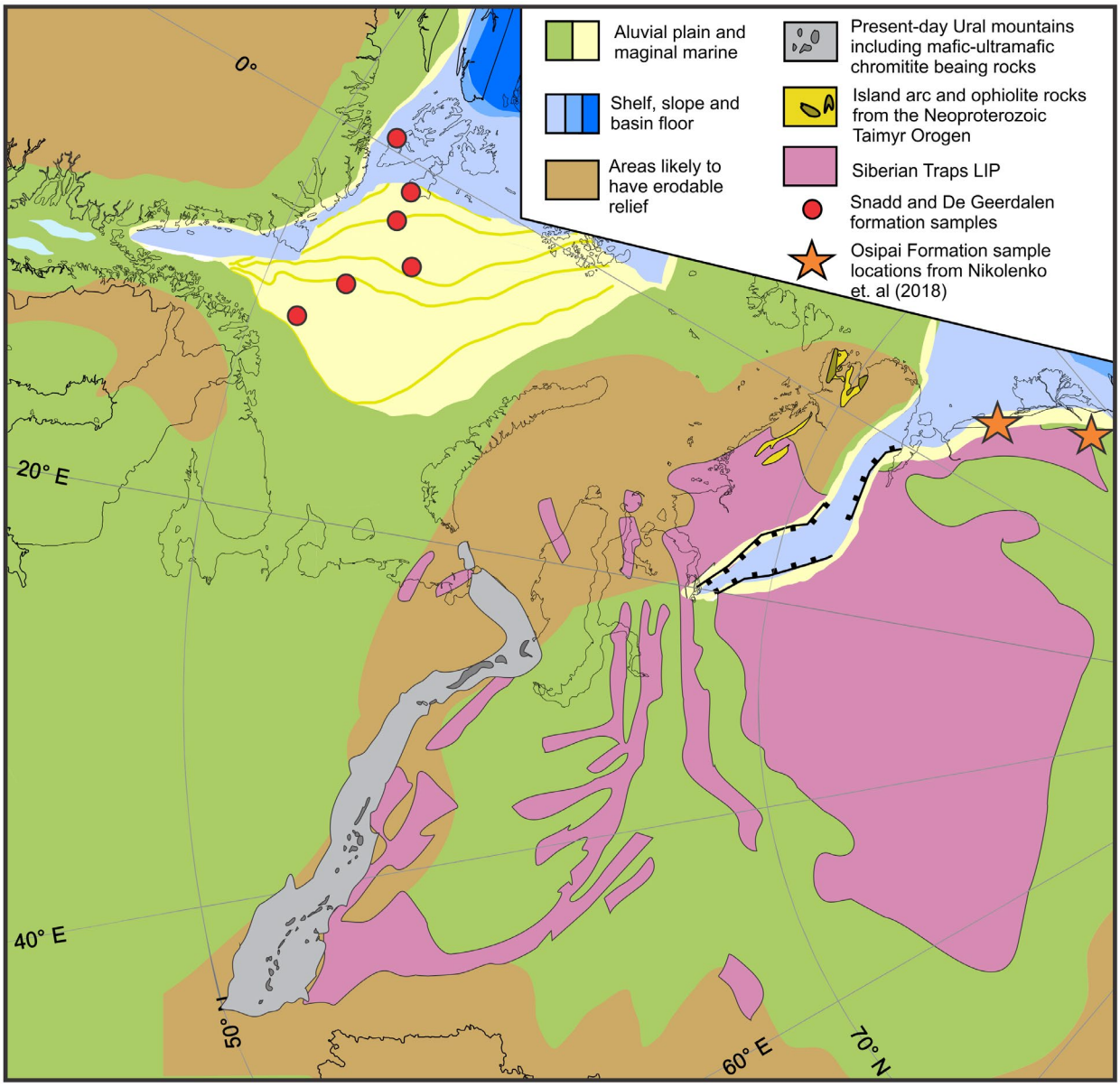

FIGURE 8 Palaeogeographic reconstruction with outlines of the Siberian Traps LIP, the present-day Ural mountains, the Taimyr Orogen Ophiolite and sample locations from this study. The map is a modified version from Sømme et al. (2018), with the Siberian Traps LIP from Ivanov et al. (2018), the Urals from Garuti et al. (2012), the Taimyr Orogen Ophiolite map from Priyatkina et al. (2017) and Osipai Formation sample locations from Nikolenko et al. (2018). The Osipai Formation detrital Cr-spinel chemistry is generally consistent with a provenance from a LIP, while detrital Cr-spinel of this study is consistent with a metamorphosed ophiolitic source. Detrital zircon geochronological data from the Barents Shelf study area and the Osipai Formation appear similar and contain the same ~235 Ma peak (Bue & Andresen, 2014; Fleming et al., 2016; Letnikova et al., 2014; Soloviev et al., 2015). The different interpretations reached based on detrital Cr-spinel chemical and zircon geochronological data thus exemlify the value of considering more than one mineral in provenance studies

possible to detect using this method alone. While Cr-spinel mineral compositions provide valuable information, integration with other methods is essential for an optimal provenance interpretation, an opinion shared by, for example, Bónová et al. (2018).

A comparison between the published data from the Osipai Formation and the Snadd and De Geerdalen formations on the Barents Shelf shows that detrital Cr-spinel chemical data can add relevant source-discriminating information. In this case, detrital zircon age distributions are unable to distinguish the different sources for these formations, while detrital Cr-spinel compositions strongly suggest influx of sediments from the Siberian Traps LIP and the Uralian Orogen respectively. In the palaeogeographic reconstruction with Siberian Traps LIP and Ural overlays presented in Figure 8, the detrital Cr-spinel compositions in both areas are consistent with the nearest potential Cr-spinel source. Further work on Cr-spinel-based provenance

is likely to increase our understanding of Triassic Arctic geology and, with increased access to microanalytical techniques, is likely to become an important tool by which interpretations based on detrital zircon data can be augmented (e.g. Duparc, Dare, Cousineau, & Goutier, 2016).

7.2 | Mineral stability in sediments and recycling

In this study we have stipulated that Cr-spinel is stable in sediments, as indicated by Morton and Hallsworth (1999). We have no observations of diagenetically altered Cr-spinel in our case study, although we cannot exclude the possibility of diagenetic alteration as this topic is still little studied and poorly understood. As with other minerals stable in sediments, there is a potential for Cr-spinel recycling over time. In our case study, with an established provenance of relatively young sources, the impact of such recycling may be limited, although there is potential for at least one erosional and depositional cycle. Research into the long-term chemical stability of detrital Cr-spinel, both under diagenetic and metamorphic conditions, would help determine the recycling potential of the mineral and simultaneously improve the reliability of detrital Cr-spinel provenance analyses.

Future studies focused on petrographic characteristics of detrital Cr-spinel, as well as mineral fertility studies, could be feasible approaches to aid Cr-spinel-based provenance interpretation. The added information could help assess recycling histories and group different Cr-spinel grains, akin to cathodoluminescence imaging of zircon. Grouping based on rounding is, for example, essential in the study of Nikolenko et al. (2018). Identification of primary and recycled material could help test the regional tectonic model hypothesised by Flowerdew et al. (2019) who suggest a Snadd formation provenance from recycled Uralian Orogen foreland sediments. Future work on the fertility of different kinds of Cr-spinel in potential source rocks would also significantly help interpretation of detrital Cr-spinel data. Chromitite is, for example, likely to contribute differently compared to disseminated Cr-spinel in co-existing rocks.

7.3 | Cr-spinel provenance; the importance of trace element compositions

The novel contribution in this study is the application of trace element chemistry in detrital Cr-spinel provenance analysis. While several previous provenance studies have applied EPMA-derived Cr-spinel compositional data, the addition of trace element compositions gives significant information about the source region and help provenance interpretations. These additional data allow the identification of metamorphic alteration of detrital Cr-spinel grains that appear unaltered when assessed only on major and minor element compositions.

The Cr-spinel compositions generally plot within the ophiolite and Supra-Subduction-Zone Peridotite fields in conventional diagrams based on major element cation compositions (Figures 2–5) (Barnes & Roeder, 2001; Kamenetsky et al., 2001). This interpretation is, however, based on data that overlap different compositional fields. The various discrimination diagrams also indicate slightly different petrogenesis for the same data (e.g. Figure 2 vs. Figures 3 and 4). Wide compositional fields complicate interpretations as data only plot in limited areas and not over the entire distributional fields. Major element-based compositional distributions of metamorphosed Cr-spinel, such as those by Suita and Strieder (1996) and Colás et al. (2014), add additional compositional fields that are both large and overlapping.

When working on detrital Cr-spinel, several of the contextual tools of conventional magmatic or metamorphic petrology, such as mineral texture and surrounding geology, is unavailable. This necessitates interpretation of the chemical data on its own. Ninety per cent of the major element cations of our case study, as seen in Figures 2 and 3, plot within the ophiolite distribution field. The few grains corresponding to metamorphic rims of Cr-spinel indicate a small metamorphic detrital contribution. A significant proportion of the Cr-spinel analyses plotting within the ophiolite field also plot within other possible distribution fields, e.g. island arcs and continental intrusions. With the issues of large and overlapping distribution fields in the conventional major element compositional plots, additional source-discriminating information will significantly improve the robustness of interpretations. The most likely interpretation based on the Cr-spinel major element compositions available from the Barents Shelf is, however, derivation from an ophiolitic source, with a few grains indicating a metamorphic history.

We can deduce a more complex source-rock history when adding trace element data, as they seem to be more sensitive to the effects of metamorphic alteration. In our case, the trace element compositions are compatible with metamorphically altered Cr-spinel. The trace element compostions are different from those of layered intrusions (González-Jiménez et al., 2015 and references therein), with only V and Sc concentrations similar to Cr-spinel from layered intrusions. Fe^{3+} concentration seems to be a good indicator of ophiolitic origin, while the trace element data illuminate the metamorphic history recorded in the Cr-spinel grains. Thus, we were able to attribute the provenance to a terrain containing metamorphosed ophiolitic units.

In the future, when more trace element compositional data from Cr spinel are available, the response of Cr-spinel to different metamorphic facies, weathering, transport and diagenesis may help establish provenance at a higher level of detail. As of now, there is an extensive literature on major and minor element compositions of Cr-spinel, while Cr-spinel trace element compositions are less developed and comparatively little data are available. Some issues arise when comparing our data to the limited amount of trace element data published, such as possible variations between regions. Another challenge is the limited knowledge about Cr-spinel compositional variation in different metamorphic environments and between different protoliths.

8 | CONCLUSIONS

The detrital Cr-spinels in the Snadd and De Geerdalen formations have major, minor and trace element compositions consistent with metamorphically altered Cr-spinel. The ultimate source of the detrital Cr-spinel is interpreted to be metamorphosed ophiolite-related mafic–ultramafic rocks in the Uralian Orogen. As all analysed Cr-spinel grains show a consistent metamorphic signature, a source contribution from rocks containing unaltered Cr-spinel appears not to be present, excluding the Siberian Traps LIP and contemporaneous volcanism as possible sources. The large degree of consistency between samples shows a continuation of the same sediment erosion, transport and depositional system over considerable time and distance.

Application of trace elements, in addition to major and minor elements, to identify Cr-spinel provenance was essential in order to generate a plausible interpretation of provenance in this study. Conventional major and minor element-based plots could less convincingly indicate petrogenesis, mainly due to large and overlapping compositional fields associated with different tectonic environments. By adding trace element data, we were able to identify chemical compositions consistent with metamorphic alteration of Cr-spinel mineral cores in ophiolites. The addition of trace element data significantly helped the provenance interpretation of the detrital Cr-spinel as it allowed exclusion of other possible spinel sources and added source rock-sensitive information.

ACKNOWLEDGEMENTS

We would like to thank the journal reviewers Michael J. Flowerdew, Akihiro Tamura and one anonymous reviewer. Their insightful comments have significantly improved the quality of this contribution. Furthermore, we wish to thank Thomas Ulrich at Aarhus University for his help with the LA–ICP–MS data collection, Dan MacDonald at Dalhousie University for help and assistance with the EPMA operation and data collection, Anette Granseth (NTNU) for her insight in data visualisation and Anna Pryadunenko (NTNU) for helpful discussions about Cr-spinel chemistry.

CONFLICT OF INTEREST

There is no conflic of interest concerning this contribution.

PEER REVIEW

The peer review history for this article is available at https://publons.com/publon/10.1111/bre.12502.

DATA AVAILABILITY STATEMENT

The data that support the findings of this study are provided in the supplementary material.

ORCID

Trond Svånå Harstad https://orcid.org/0000-0003-2313-4602
Trond Slagstad https://orcid.org/0000-0002-8059-2426

REFERENCES

Azizi, S. H. H., Rezaee, P., Jafarzadeh, M., Meinhold, G., Harami, S. R. M., & Masoodi, M. (2018). Evidence from detrital chrome spinel chemistry for a Paleo-Tethyan intra-oceanic island-arc provenance recorded in Triassic sandstones of the Nakhlak Group, Central Iran. *Journal of African Earth Sciences*, *143*, 242–252. https://doi.org/10.1016/j.jafrearsci.2018.03.006

Barnes, S. J., & Roeder, P. L. (2001). The range of spinel compositions in terrestrial mafic and ultramafic rocks. *Journal of Petrology*, *42*, 2279–2302. https://doi.org/10.1093/petrology/42.12.2279

Bónová, K., Mikuš, T., & Bóna, J. (2018). Is Cr-spinel geochemistry enough for solving the provenance dilemma? Case study from the palaeogene sandstones of the Western Carpathians (Eastern Slovakia). *Minerals*, *8*, 543. https://doi.org/10.3390/min8120543

Bue, E. P., & Andresen, A. (2014). Constraining depositional models in the Barents Sea region using detrital zircon U-Pb data from mesozoic sediments in Svalbard. *Geological Society, London, Special Publications*, *386*, 261–279. https://doi.org/10.1144/SP386.14

Bugge, T., Elvebakk, G., Fanavoll, S., Mangerud, G., Smelror, M., Weiss, H. M., … Nilsen, K. (2002). Shallow stratigraphic drilling applied in hydrocarbon exploration of the Nordkapp Basin, Barents Sea. *Marine and Petroleum Geology*, *19*, 13–37. https://doi.org/10.1016/S0264-8172(01)00051-4

Colás, V., González-Jiménez, J. M., Griffin, W. L., Fanlo, I., Gervilla, F., O'Reilly, S. Y., … Proenza, J. A. (2014). Fingerprints of metamorphism in chromite: New insights from minor and trace elements. *Chemical Geology*, *389*, 137–152. https://doi.org/10.1016/j.chemgeo.2014.10.001

Cookenboo, H., Bustin, R., & Wilks, K. (1997). Detrital chromian spinel compositions used to reconstruct the tectonic setting of provenance; Implications for orogeny in the Canadian Cordillera. *Journal of Sedimentary Research*, *67*, 116–123.

Droop, G. (1987). A general equation for estimating Fe^{3+} concentrations in ferromagnesian silicates and oxides from microprobe analyses, using stoichiometric criteria. *Mineralogical Magazine*, *51*, 431–435.

Duparc, Q., Dare, S. A., Cousineau, P. A., & Goutier, J. (2016). Magnetite chemistry as a provenance indicator in archean metamorphosed

sedimentary rocks. *Journal of Sedimentary Research*, *86*, 542–563. https://doi.org/10.2110/jsr.2016.36

Dupuis, C., & Beaudoin, G. (2011). Discriminant diagrams for iron oxide trace element fingerprinting of mineral deposit types. *Mineralium Deposita*, *46*, 319–335. https://doi.org/10.1007/s00126-011-0334-y

Evans, B. W., & Frost, B. R. (1976). Chrome-spinel in progressive metamorphism—A preliminary analysis. In T. N. Irvine (Eds.), *Chromium: Its physicochemical behavior and petrologic significance* (pp. 959–972). Pergamon. https://doi.org/10.1016/B978-0-08-019954-2.50020-2

Fanlo, I., Gervilla, F., Colás, V., & Subías, I. (2015). Zn-, Mn-and Co-rich chromian spinels from the Bou-Azzer mining district (Marocco): Constraints on their relationship with the mineralizing process. *Ore Geology Reviews*, *71*, 82–98.

Fleming, E. J., Flowerdew, M. J., Smyth, H. R., Scott, R. A., Morton, A. C., Omma, J. E., … Whitehouse, M. J. (2016). Provenance of Triassic sandstones on the southwest Barents Shelf and the implication for sediment dispersal patterns in northwest Pangaea. *Marine and Petroleum Geology*, *78*, 516–535. https://doi.org/10.1016/j.marpetgeo.2016.10.005

Flowerdew, M. J., Fleming, E. J., Morton, A. C., Frei, D., Chew, D. M., & Daly, J. S. (2019). Assessing mineral fertility and bias in sedimentary provenance studies: Examples from the Barents Shelf. *Geological Society, London, Special Publications*, *484*(SP484), 411. https://doi.org/10.1144/SP484.11

Garuti, G., Pushkarev, E. V., Thalhammer, O. A., & Zaccarini, F. (2012). Chromitites of the Urals (part 1): Overview of chromite mineral chemistry and geo-tectonic setting. *Ofioliti*, *37*, 27–53.

Glørstad-Clark, E., Faleide, J. I., Lundschien, B. A., & Nystuen, J. P. (2010). Triassic seismic sequence stratigraphy and paleogeography of the western Barents Sea area. *Marine and Petroleum Geology*, *27*, 1448–1475. https://doi.org/10.1016/j.marpetgeo.2010.02.008

González-Jiménez, J. M., Camprubí, A., Colás, V., Griffin, W. L., Proenza, J. A., O'Reilly, S. Y., … Talavera, C. (2017). The recycling of chromitites in ophiolites from southwestern North America. *Lithos*, *294*, 53–72. https://doi.org/10.1016/j.lithos.2017.09.020

González-Jiménez, J. M., Griffin, W. L., Proenza, J. A., Gervilla, F., O'Reilly, S. Y., Akbulut, M., … Arai, S. (2014). Chromitites in ophiolites: How, where, when, why? Part II. The Crystallization of Chromitites. *Lithos*, *189*, 140–158. https://doi.org/10.1016/j.lithos.2013.09.008

González-Jiménez, J. M., Locmelis, M., Belousova, E., Griffin, W. L., Gervilla, F., Kerestedjian, T. N., … Sergeeva, I. (2015). Genesis and tectonic implications of podiform chromitites in the metamorphosed ultramafic massif of Dobromirtsi (Bulgaria). *Gondwana Research*, *27*, 555–574. https://doi.org/10.1016/j.gr.2013.09.020

Henriksen, E., Bjørnseth, H., Hals, T., Heide, T., Kiryukhina, T., Kløvjan, O., … Sollid, K. (2011). Uplift and erosion of the greater Barents Sea: Impact on prospectivity and petroleum systems. *Geological Society, London, Memoirs*, *35*, 271–281.

Hölttä, P., Balagansky, V., Garde, A. A., Mertanen, S., Peltonen, P., Slabunov, A., … Whitehouse, M. (2008). Archean of Greenland and Fennoscandia. *Episodes*, *31*, 13–19. https://doi.org/10.18814/epiiugs/2008/v31i1/003

Irvine, T. (1965). Chromian spinel as a petrogenetic indicator: Part 1. Theory. *Canadian Journal of Earth Sciences*, *2*, 648–672. https://doi.org/10.1139/e65-046

Ivanov, A. V., Demonterova, E. I., Savatenkov, V. M., Perepelov, A. B., Ryabov, V. V., & Shevko, A. Y. (2018). Late Triassic (Carnian) lamproites from Noril'sk, polar Siberia: Evidence for melting of the recycled Archean crust and the question of lamproite source for some placer diamond deposits of the Siberian Craton. *Lithos*, *296*, 67–78. https://doi.org/10.1016/j.lithos.2017.10.021

Jochum, K. P., Stoll, B., Herwig, K., Willbold, M., Hofmann, A. W., Amini, M., …Woodhead, J. D. (2006). MPI-DING reference glasses for in situ microanalysis: New reference values for element concentrations and isotope ratios. *Geochemistry, Geophysics, Geosystems*, *7*, Q02008.

Kamenetsky, V. S., Crawford, A. J., & Meffre, S. (2001). Factors controlling chemistry of magmatic spinel: An empirical study of associated olivine, Cr-spinel and melt inclusions from primitive rocks. *Journal of Petrology*, *42*, 655–671. https://doi.org/10.1093/petrology/42.4.655

Khudoley, A. K., Sobolev, N. N., Petrov, E. O., Ershova, V. B., Makariev, A. A., Makarieva, E. V., … Sobolev, P. O. (2019). A reconnaissance provenance study of Triassic-Jurassic clastic rocks of the Russian Barents Sea. *GFF*, *144*, 263–271. https://doi.org/10.1080/11035897.2019.1621372

Klausen, T. G., Müller, R., Slama, J., & Helland-Hansen, W. (2017). Evidence for Late Triassic provenance areas and Early Jurassic sediment supply turnover in the Barents Sea Basin of northern Pangea. *Lithosphere*, *9*, 14–28. https://doi.org/10.1130/L556.1

Klausen, T. G., Nyberg, B., & Helland-Hansen, W. (2019). The largest delta plain in earth's history. *Geology*, *47*, 470–474. https://doi.org/10.1130/G45507.1

Klausen, T. G., Ryseth, A. E., Helland-Hansen, W., Gawthorpe, R., & Laursen, I. (2015). Regional development and sequence stratigraphy of the Middle to Late Triassic Snadd formation, Norwegian Barents Sea. *Marine and Petroleum Geology*, *62*, 102–122. https://doi.org/10.1016/j.marpetgeo.2015.02.004

Letnikova, E., Izokh, A., Nikolenko, E., Pokhilenko, N., Shelestov, V., Hilen, G., & Lobanov, S. (2014). Late Triassic high-potassium trachitic volcanism of the northeast of the Siberian platform: Evidence in the sedimentary record. *Doklady Earth Sciences*, Springer, *459*, 1344–1347. https://doi.org/10.1134/S1028334X14110221

Lundschien, B. A., Høy, T., & Mørk, A. (2014). Triassic hydrocarbon potential in the northern Barents Sea; Integrating Svalbard and stratigraphic core data. *Norwegian Petroleum Directorate Bulletin*, *11*, 3–20.

Midwinter, D., Hadlari, T., Davis, W., Dewing, K., & Arnott, R. (2016). Dual provenance signatures of the Triassic northern Laurentian margin from detrital-zircon U-Pb and Hf-isotope analysis of Triassic-Jurassic strata in the Sverdrup Basin. *Lithosphere*, *8*, 668–683. https://doi.org/10.1130/L517.1

Miller, E. L., Soloviev, A. V., Prokopiev, A. V., Toro, J., Harris, D., Kuzmichev, A. B., & Gehrels, G. E. (2013). Triassic river systems and the paleo-pacific margin of northwestern Pangea. *Gondwana Research*, *23*, 1631–1645. https://doi.org/10.1016/j.gr.2012.08.015

Moore, A. C., & Qvale, H. (1977). Three varieties of alpine-type ultramafic rocks in the Norwegian Caledonides and basal gneisis complex. *Lithos*, *10*, 149–161. https://doi.org/10.1016/0024-4937(77)90042-1

Mørk, A., Knarud, R., & Worsley, D. (1982) Depositional and diagenetic environments of the Triassic and Lower Jurassic succession of Svalbard. In A. F. Embry, & H. R. Balkwill (Eds.), *Arctic geology and geophysics* (pp. 371–398). Canadian Society of Petroleum geology.

Mørk, M. B. E. (1999). Compositional variations and provenance of Triassic sandstones from the Barents Shelf. *Journal of Sedimentary Research*, *69*, 690–710. https://doi.org/10.2110/jsr.69.690

Mørk, M. B. E. (2013). Diagenesis and quartz cement distribution of low-permeability Upper Triassic-Middle Jurassic reservoir sandstones, Longyearbyen CO_2 lab well site in Svalbard, Norway. *AAPG Bulletin*, *97*, 577–596. https://doi.org/10.1306/10031211193

Morton, A. C., & Hallsworth, C. R. (1999). Processes controlling the composition of heavy mineral assemblages in sandstones. *Sedimentary Geology*, *124*, 3–29. https://doi.org/10.1016/S0037-0738(98)00118-3

Nikolenko, E., Logvinova, A., Izokh, A., Afanas'ev, V., Oleynikov, O., & Biller, A. Y. (2018). Cr-spinel assemblage from the Upper Triassic gritstones of the northeastern Siberian platform. *Russian Geology and Geophysics*, *59*, 1348–1364. https://doi.org/10.1016/j.rgg.2018.09.011

Pagé, P., & Barnes, S. J. (2009). Using trace elements in chromites to constrain the origin of podiform chromitites in the Thetford Mines Ophiolite, Québec, Canada. *Economic Geology*, *104*, 997–1018.

Paton, C., Hellstrom, J., Paul, B., Woodhead, J., & Hergt, J. (2011). Iolite: Freeware for the visualisation and processing of mass spectrometric data. *Journal of Analytical Atomic Spectrometry*, *26*, 2508–2518. https://doi.org/10.1039/c1ja10172b

Priyatkina, N., Collins, W. J., Khudoley, A., Zastrozhnov, D., Ershova, V., Chamberlain, K., … Proskurnin, V. (2017). The proterozoic evolution of northern Siberian Craton margin: A comparison of U-Pb–Hf signatures from sedimentary units of the Taimyr orogenic belt and the Siberian platform. *International Geology Review*, *59*, 1632–1656. https://doi.org/10.1080/00206814.2017.1289341

Puchkov, V. N. (2009). The evolution of the Uralian Orogen. *Geological Society, London, Special Publications*, *327*, 161–195. https://doi.org/10.1144/SP327.9

Riis, F., Lundschien, B. A., Høy, T., Mørk, A., & Mørk, M. B. E. (2008). Evolution of the Triassic Shelf in the northern Barents Sea region. *Polar Research*, *27*, 318–338. https://doi.org/10.1111/j.1751-8369.2008.00086.x

Rui, H., Jiao, J., Xia, M., Yang, J., & Xia, Z. (2019). Origin of chromitites in the Songshugou Peridotite Massif, Qinling Orogen (Central China): Mineralogical and geochemical evidence. *Journal of Earth Science*, *30*, 476–493. https://doi.org/10.1007/s12583-019-1227-8

Säntti, J., Kontinen, A., Sorjonen-Ward, P., Johanson, B., & Pakkanen, L. (2006). Metamorphism and chromite in serpentinized and carbonate-silica-altered peridotites of the Paleoproterozoic Outokumpu-Jormua Ophiolite Belt, Eastern Finland. *International Geology Review*, *48*, 494–546. https://doi.org/10.2747/0020-6814.48.6.494

Soloviev, A., Zaionchek, A., Suprunenko, O., Brekke, H., Faleide, J., Rozhkova, D., … Hourigan, J. (2015). Evolution of the provenances of Triassic rocks in Franz Josef Land: U/Pb LA-ICP-MS dating of the detrital zircon from well Severnaya. *Lithology Mineral Resources*, *50*, 102–116. https://doi.org/10.1134/S0024490215020054

Sømme, T., Doré, A., Lundin, E., & Tørudbakken, B. (2018). Triassic-paleogene paleogeography of the Arctic: Implications for sediment routing and basin fill. *AAPG Bulletin*, *102*, 2481–2517. https://doi.org/10.1306/05111817254

Stensland, H., Auset, M., Elvebakk, G., & Mørk, M. B. E. (2013).Palaeosols and Eogenesis of Triassic Sediments from Shallow Cores at the Bjarmeland Platform and in the Nordkapp Basin, Southwestern Barents Sea. Abstract and Poster, Norsk Geologisk Forenings Landsmøte i Oslo.

Suita, M. T. D. F., & Strieder, A. J. J. (1996). Cr-spinels from Brazilian mafic-ultramafic complexes: Metamorphic modifications. *International Geology Review*, *38*, 245–267. https://doi.org/10.1080/00206819709465333

Vigran, J. O., Mangerud, G., Mørk, A., & Hochuli, P. A. (2014). Palynology and geology of the Triassic Succession of Svalbard and the Barents Sea. *Geological Survey of Norway Special Publication*, *14*, 270.

Zhang, X., Pease, V., Carter, A., Kostuychenko, S., Suleymanov, A., & Scott, R. (2017). Timing of exhumation and deformation across the Taimyr fold-thrust belt: Insights from apatite fission track dating and balanced cross-sections. *Geological Society, London, Special Publications*, *460*(SP460), 463. https://doi.org/10.1144/SP460.3

Zhang, X., Pease, V., Carter, A., & Scott, R. (2017). Reconstructing Palaeozoic and Mesozoic tectonic evolution of Novaya Zemlya: Combing geochronology and thermochronology. *Geological Society, London, Special Publications*, *460*(SP460), 413. https://doi.org/10.1144/SP460.13

Zhang, X., Pease, V., Skogseid, J., & Wohlgemuth-Ueberwasser, C. (2016). Reconstruction of tectonic events on the northern Eurasia margin of the Arctic, from U-Pb detrital zircon provenance investigations of late Paleozoic to Mesozoic sandstones in southern Taimyr Peninsula. *Bulletin*, *128*, 29–46.

SUPPORTING INFORMATION

Additional Supporting Information may be found online in the Supporting Information section.

How to cite this article: Harstad TS, Mørk MBE, Slagstad T. The importance of trace element analyses in detrital Cr-spinel provenance studies: An example from the Upper Triassic of the Barents Shelf. *Basin Res*. 2021;33:1017–1032. https://doi.org/10.1111/bre.12502